Egypt. J. Chem. **Vol. 60**, No.3, pp. 379 -394 (2017)

Preparation and Characterization of Nano Structured Pt-MOx/C for Oxygen Reduction Reaction in Acidic Medium

K.M. El−Khatib[1]*, Amani E. Fetohi[1], R.S. Amin[1] and R.M. Abdel Hameed[2]
[1]Chemical Engineering Department, National Research Center,El-Buhous st.,Dokki and [2]Chemistry Department, Faculty of Science, Cairo University, Giza, Egypt.

Pt-MOx/C (M = Ti, Ce or Zr) electrocatalysts was prepared for the purpose of developing a cheap and efficient electrocatalysts for oxygen reduction reaction (ORR) using a mixture of ethylene glycol and sodium borohydride (EG + $NaBH_4$) as areducing agent. Pt/C was studied for estimation of metal oxides effect.Pt-CeO_2/C-1 was prepared through single reducing agent ethylene glycol for studying the effect of changing the reducing agent on the activity of electrocatalysts toward ORR and for studying ORR kinetics. The electrocatalytic activity of the prepared electrocatalysts towards (ORR) was evaluated by cyclic voltammetry (CV) and linear sweep voltammetry (LSV) on a rotating disc electrode (RDE). Pt-ZrO_2 /C shows the best activity towards ORR among the studied electrocatalysts; the oxygen reduction current density for it is about 5 times; (5.84 $mAcm^{-2}$) as that of Pt/C (1.26 $mAcm^{-2}$). Pt-CeO_2/C showed better ORR activity (2.24 $mAcm^{-2}$) than Pt-CeO_2/C-1(1.58 $mAcm^{-2}$) indicating the great effect of changing the reducing agent not only on the electrocatalyst behavior towards ORR but also its particle size and the metal content of the resultant electrocatalysts. Oxygen reduction mechanism for Pt-CeO_2/C and Pt-CeO_2/C-1 was evaluated using through Koutecky-Levich, they showed first-order kinetics with ORR not controlled solely by diffusion. XRD, EDX and TEM analyses were used to characterize the prepared electrocatalyst.

Keywords: Oxygen reduction reaction, platinum nanoparticles, metal oxides, rotating disk electrode.

Introduction

Oxygen reduction reaction (ORR) is one of the most important electrocatalytic reactions because of its role in corrosion of metals and electrochemical energy conversion especially in the field of fuel cells applications[1]. The cell voltage values of fuel cells are limited due to the slowness of ORR at the cathode. The most used electrocatalyst for ORR is platinum which is highly active chemically stable, but Pt is expensive and limited in the world's supply; this results in difficulty of widespread commercialization of the fuel cell technology. So, research efforts in the development of cathode electrocatalysts have been focused on reducing the Pt content or replacing it with less expensive materials with maintaining high ORR activity[2], so getting electrocatalysts in which transition metals have been alloyed with noble metals is a need[3-5].

The principal problems that inhibit direct methanol fuel cells (DMFCs) commercialization are: development of a highly active and CO-tolerant anode catalysts and the overcoming of the oxygen reduction reaction (ORR) slowness at the cathode [6].Considering that Pt catalysts alone we face a problem of the slowness of ORR which is due to the formation of - OH species at +0.8 V that inhibits further reduction of oxygen and hence results in loss of performance[7] .So, composite Pt-based electrocatalysts containing rare earth oxides have shown a number of characteristics that make them promising for catalytic studies due to the harmonic electronic effect in combining metal oxides, carbon and Pt. Strong d-d-Metal-Support Interaction of hyper-d-electronic metal with mostly hypo-d-oxide (TiO_2, ZrO_2, HfO_2) implies that the d-d-metal-oxide interaction is in accordance with the bonding strength which results in weakening of intermediate chemisorptive bonds (M-H, M-CO) [8-12].Among the studied metal oxides, CeO_2 is predominant in the applications as catalyst support[13-17]. CeO_2 is a fluorite oxide whose cations can switch between +3 and +4 oxidation states, here the oxide acts as an oxygen buffer

*Corresponding author e-mail: kamelced@hotmail.com
DOI :10.21608/ejchem.2017.753.1022

to control oxygen concentration at the catalyst surface. This may be due to the enhancement of the interaction between Pt and ceria for the catalytic activities of Pt[18, 19]. Cerium oxide nanoparticles were in-situ grown on reduced graphene oxide (rGO) through thermal treatment of the Ce^{3+}-doped graphene oxide(GO) under nitrogen atmosphere. The nano composites show electrocatalytic activity toward the oxygen reduction reaction (ORR) in alkaline solution. Especially, the cerium oxide nanoparticles/rGO nanocomposites treated at 750 C possess excellent electrocatalytic ability with a dominating four-electron pathway[20].

TiO_2 is promising because of its good electrochemical properties, chemical stability and non-toxic nature[21]. Pt-TiO_2/C shows improved stability in polymer electrolyte membrane fuel cells (PEMFCs) compared with Pt/C[22].In spite of the amount of titanium dioxide and the crystalline phase (TiO_2 anatase/rutile phase) it was found that, it modifies the strength of the interaction between the substrate and the metal nanoparticles[23, 24]. The good effect of addition TiO_2 may be attributed to two factors which are: the changes in the Pt-d electronic properties and the geometric effect that leads to the Pt-Pt bonding distance contraction and hence results in a sensible improvement of the electrochemical reactions[25, 26].Titanium oxide-based cathode, synthesized from oxy-titanium tetra-pyrazinoporphyrazine by the oxidation under a low partial pressure of oxygen using carbon nano-tubes as a support, showed high reactivity in the four–electron reduction of oxygen[27]. Platinum nanoparticles (Pt NPs) have been anchored by photo deposition on titanium oxide (TiO_2) matrix which is formed via titanium isopropoxide hydrolysis on cup–stacked carbon nanotubes (CSCNT) in isopropanol, the resultant composite Pt catalyst was tested for oxygen reduction reaction (ORR) in acidic media and the results revealed that the anchoring of Pt NPs on the TiO_2 support material deposited on CSCNT is an effective way to enhance the ORR activity of Pt NPs[28]. A 15 wt.% Pt-based catalyst was developed on a mixture of titanium suboxides, with an excess of the Ti3O5 phase, doped with Mo, as a Ti_3O_5-Mo without carbon support and compared to a commercial 20 wt.% Pt/C (E-TEK). The Pt/Ti_3O_5-Mo catalyst shows an excellent electroactivity and stability toward the ORR, reaching a performance of 73.3 mA mg^{-1}, nearly twice as that of the commercial Pt/C, with a current density of 1.1 mA cm^{-2} at 0.9 V vs RHE, and an half-wave potential of 0.86 V vs RHE [29]. Pt/ZrO_2@CNx has been synthesized by forming a highly conductive nitrogen−doped carbon layer on the surface of ZrO_2 (ZrO_2@CNx) the final step is the Pt nanoparticles deposition. The Pt/ZrO_2@CNx catalyst showed a high electrocatalytic activity for the oxygen reduction reaction (ORR)[30]. A two−step method has been used by G. Liu et al. to prepare Pt_4ZrO_2/C catalyst as a cathode catalyst in a high temperature PEMFC based on H_3PO_4 doped polybenzimidazole (PBI) to investigate the cell performance[31]. Cobalt oxide (Co_3O_4) nanocubes were incorporated into reduced graphene oxide (RGO) using a simple single-step hydrothermal reaction for an electrocatalytic oxygen reduction reaction (ORR). The RGO@Co_3O_4 nano hybrid with 4 wt% of graphene oxide modified glassy carbon (GC) electrode exhibited better electrocatalytic activity when compared to the other controlled modified electrodes and commercial Pt/C catalyst for the ORR in an alkaline medium[32]. Bifunctional electrocatalysts series composed of nitrogen-doped grapheme cobalt oxide nanoparticles nano-hybrids (Co-N/G) are fabricated through one-pot hydrothermal synthesis, The optimized Co-N/G catalyst consists of the highest contents of pyridinic nitrogen and CoO, efficiently catalyze both ORR and OER[33].

Microwave-assisted technology has been widely used for preparing many nanomaterials because it is a quick, simple, homogeneous and efficient method [34-36]. Smaller particles were formed when microwave irradiation method was adopted. It was reported that Pt particles with about 3-4 nm size exhibited a higher mass electrocatalytic activity for oxygen reduction [37, 38]. Pt–Ru particles with 3 nm size displayed the highest mass catalytic activity for methanol electrooxidation [39]. So as a direct result, microwave irradiation method is applicable in different areas namely; materials synthesis, food drying, microwave-induced catalysis and plasma chemistry [40-43].

The present work aims to study physical and electrochemical behavior of Pt-MOx/C electrocatalysts, where MOx refers to TiO2, CeO2 and ZrO_2 in order to develop a cheaper and more efficient electrocatalyst for oxygen reduction reaction. Pt/C has been studied to evaluate the metal oxide effect; Pt-CeO_2/C-1 has been studied to evaluate the effect of the changing of the used reducing agent on the behavior of the prepared electrocatalyst.

Experimental

Catalyst synthesis

All the reagents in this synthesis were in analytical grade (Sigma-Aldrich) and used without further purification. Double distilled water was used in all aqueous solutions preparation and washing. According to this preparation method, we have synthesized Pt-TiO_2/C, Pt-CeO_2/C and Pt-ZrO_2/C electrocatalysts using titanium (IV) oxide (TiO_2), cerium (IV) oxide (CeO_2) and zirconium (IV) oxide (ZrO_2), respectively through two steps. The first step involved the synthesis of MO_x/C powders via solid state reaction under intermittent microwave heating, while the second step is platinum loading on MO_x/C surfaces. To prepare MO_x/C, a fixed amount of titanium (IV) oxide (TiO_2), cerium (IV) oxide (CeO_2) or zirconium (IV) oxide (ZrO_2) [5 wt.%] well dispersed over carbon black Vulcan XC−72R using a mixture of second distilled water and isopropanol in the ratio of (1:1). This suspension was stirred using magnetic stirrer for 30 min and heated into a microwave oven (Caira CA-MW1025, touch pad digital control, 50 MHz, 1400 W) in six cycles; each cycle was 20 s on and 60 s off. The next step is the filtration of the mixture and washing it with double distilled water for 6 times, the last step is drying in an air oven at 80°C for 6 h. Reduction of platinum on the prepared MO_x/C powders is done through modified microwave-assisted polyol process in which H_2PtCl_6 solution was added to a suspension of MO_x/C powder in distilled water with adjusting Pt loading at 25 wt.%. For this step, a mixture of ethylene glycol and sodiumborohydride (EG + $NaBH_4$) were used (in this case the electrocatalysts are assigned as Pt-MO_x/C). pH of the solution was adjusted at 10 using 0.4 M KOH in ethylene glycol to induce the formation of small and uniform Pt nanoparticles. This mixture was then heated into the microwave oven for 50 s in one continuous mode. Pt-MO_x/C powder was then filtered, washed and dried. Pt-CeO_2/C-1was prepared via the same procedure using single reducing agent ethylene glycol (EG) for studying the effect of changing the reducing agent during the preparation process.

Physical characterization

XRD, TEM and EDX analyses are used to describe Pt/C and the mentioned Pt-MOx/C electrocatalysts physically. Specifications of devices used to evaluate these types of analyses are: a RigakuD/MAX-PC 2500 X-ray diffractometer equipped with Ni filtered Cu Ka as the radiation source. The tube current was 40 mA with a voltage of 40 kV to evaluate the crystalline structure of the prepared electrocatalysts. TEM and EDX analyses was performed using JEOL-JEM 2010 transmission electron microscope that operated at an accelerating voltage of 160 kV

Electrochemical measurements

Voltamaster 6 potentiostat and Rotating Disc Electrode (RDE) were employed for the electrochemical measurements. It is connected to a personal computer as data interface. Cyclic voltammetry (CV) and linear sweep voltammetry (LSV) were conducted to measure the electrocatalytic activity of the prepared Pt–MO_x/C electrocatalysts towards oxygen reduction reaction. The three electrode cell consists of Pt wire and Ag/AgCl as the counter and the reference electrodes, respectively. All the potential values in this work are referred to RHE. The working electrode was a thin film of electrocatalyst supported on glassy carbon (GC) electrode (with geometrical surface area of 0.196 cm^2) which is a part of the RDE. This GC electrode was first polished using 0.05 μm alumina powder and soft cloth then carbon-supported electrocatalyst was put on it mixed with 1 droplet of isopropanol, two consecutive droplets of 5% Nafion solution were put after isopropanol has dried, at last a second droplet of isopropanol was added, the electrocatalyst thin film was left till air drying. The catalyst loading is 0.6 mg/cm^2.

For the electrochemical active surface area (ECSA) determination experiments, they were carried out at room temperature employing 0.5 M H_2SO_4 as the electrolyte solution and three electrode system in which Hg/Hg_2SO_4/1.0 M H_2SO_4(MMS) is the reference electrode. Thirty CVs with scan rate of 50 mVs^{-1} at a potential window (-700 to 900 mV/MMS) (-80 to 1520 mV/RHE) was conducted.

All electrochemical experiments were carried out at room temperature and ambient pressure employing 0.5 M H_2SO_4 as the electrolyte solution. At first nitrogen was bubbled for 20 min. The CV scan at the 10th cycle is recorded scan rate of 50 mVs−1 with a potential window (-200 to 1000 mV/Ag/AgCl) (-1 to 1199 mV/RHE) and one LSV with scan rate of 10 mVs-1 in a potential range (1000 to-200 mV/Ag/AgCl) (1199 to-1 mV/RHE) was performed, then oxygen bubbling for 30 min, after that LSVs with different rpm values ranging between 200 rpm to 2400 rpm were performed in solution saturated with

oxygen with the same conditions as in case of LSV performed in solution saturated with nitrogen. The same conditions of CV recorded in nitrogen is repeated in case of oxygen.

Results and Discussion

Physical characterization of Pt-MOx/C electrocatalysts

Figure (1a) showed the X-ray diffraction (XRD) of Pt-TiO_2/C, Pt-CeO_2/C and Pt-ZrO_2/C electrocatalysts in comparison with that of Pt/C. The diffraction peaks of Pt(111), Pt(200) and Pt(220) appear in allelectrocatalysts. XRD pattern of Pt-CeO_2/C-1electrocatalysts shows that CeO_2 has four diffraction peaks of CeO_2 at 2θ = 28.6°, 33.1°, 47.5° and 56.3° that correspond to (111), (200), (220) and (311) diffraction planes, respectively[44].These are typical of single-phase oxides with fluorite structures. so, both Pt and CeO_2 phases exist simultaneously in Pt-CeO_2/C electrocatalyst, it was also noticed that; after introducing CeO_2 to Pt/C in Pt-CeO_2/C electrocatalyst, 2θ values are shifted in the positive direction when compared to those of Pt in Pt/C as shown in Table 1 while for Pt-ZrO_2/C electrocatalyst Pt(111), Pt(200) and Pt(220) planes are observed at 2θ = 39.765°, 45.909° and 67.682o, respectively.

Pt(111) and Pt(220) planes are shifted to higher 2θ values when compared to those of Pt/C as shown in Table 1. This is an indication for the fact that incorporation of ZrO_2 affects the crystalline lattice of platinum; no diffraction planes related to ZrO_2 phase were found. This can be due to the low concentration of ZrO_2 or partial ZrO_2 entering into Pt crystalline lattice[45-48]. For Pt-TiO_2/C electrocatalyst we can notice that; Pt(111) Pt (200) and Pt(220) diffraction planes are found to be at higher 2θ values when compared to those in Pt/C^{-1} as in Table 1 resulting in a crystal lattice contraction, it is also noticed from Fig.1 (a) that; no characteristic peak for TiO_2 is found in XRD pattern, this could be interpreted by the existence of the titanium oxide in an amorphous form[49]. Pt (200) diffraction planes of Pt-CeO_2/C-1, showed 2θ shift to higher values 47.326 when compared to that of Pt-CeO_2/C47.319 as seen from Fig.1b while the corresponding interplanar spacing parameter is constant 1.919. Pt (111) and Pt (220) diffraction planes of Pt-CeO_2/C-1 show no values, so we can conclude that introducing CeO_2 in Pt-

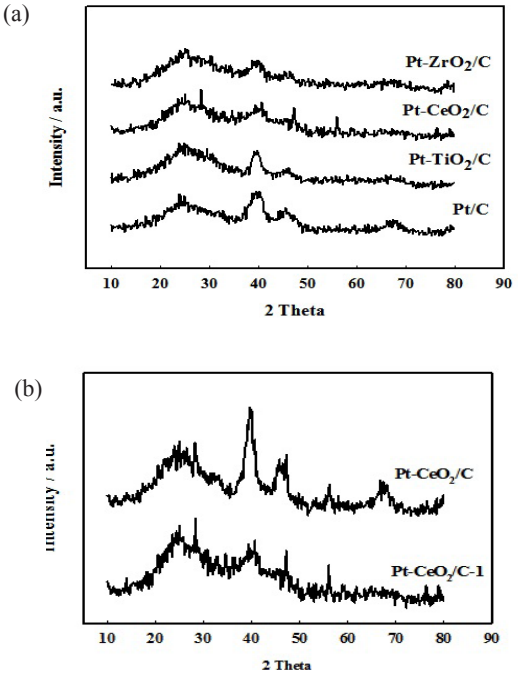

Fig.1. XRD patterns of (a) Pt/C and different Pt–MOx/C, (b) Pt-CeO_2/C and Pt-CeO_2/C-1 electrocatalysts.

TABLE 1. Variation of 2θ and d values of Pt(111), Pt(200) and Pt(220) diffraction peaks of Pt/C and different Pt–MOx/C electrocatalysts.

Electrocatalyst	Pt(111)		Pt(200)		Pt(220)		Pt crystallite size / nm
	2θ / Å	d / Å	2θ / Å	d / Å	2θ / Å	d / Å	
Pt/C	39.265	2.293	46.001	1.971	67.353	1.389	-
Pt–TiO_2/C	39.678	2.270	46.339	1.958	67.539	1.386	-
Pt–CeO_2/C	39.621	2.272	47.319	1.919	67.563	1.385	3.2
Pt–ZrO_2/C	39.765	2.264	45.909	1.975	67.682	1.383	-
Pt–CeO_2/C-1	-	-	47.326	1.919	-	-	-

CeO_2/C-1 leads to crystal lattice contraction. It was found that the Pt particle size for Pt in Pt-CeO2/C is 3.2 nm while that inPt-ZrO_2/C, Pt-TiO_2/C and Pt-CeO_2/C-1electrocatalysts could not be estimated, this phenomena is attributed to the fact that, XRD gives information about crystalline size information rather than true particle size[50].

Energy dispersive X-ray (EDX) analysis has been carried out to determine the elemental composition of the prepared Pt/C and Pt-MO_x/C electrocatalysts. Figure 2 (a-e) present the (EDX) spectra of Pt/C, Pt-TiO_2/C and Pt-CeO_2/C, Pt-ZrO_2/C and Pt-CeO_2/C-1electrocatalysts respectively. The weight and atomic percentages of different elements constituting these electrocatalysts are presented in Table 2. Wt. % of Pt was found to be 36.03 in Pt/C electrocatalyst. This percentage was increased when different MOx were introduced. All studied samples found to contain carbon, oxygen and platinum in different weight percentages. It is noticed from Table 2 that Pt-ZrO_2/C electrocatalyst showed the highest weight percentages of Pt (56.03) while Pt-CeO_2/C-1 electrocatalyst showed the lowest one (10.39). On the other hand we found that; Pt-CeO_2/C has the highest weight percentage value for the metal (here; Ce) 8.84. On studying the effect of reducing agent we can observe that, using single reducing agent (EG) decreases the Wt.% of Pt and M (Ce) while increases that of C and O. It was also noticed that the weight percentage of oxygen for electrocatalysts prepared using mixed reducing agent is low when compared to that prepared using single reducing agent.

Transmission electron microscopy (TEM) image of Pt/C electrocatalyst was shown in Fig.

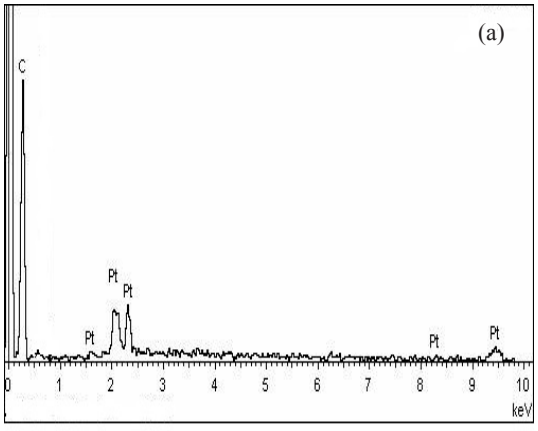

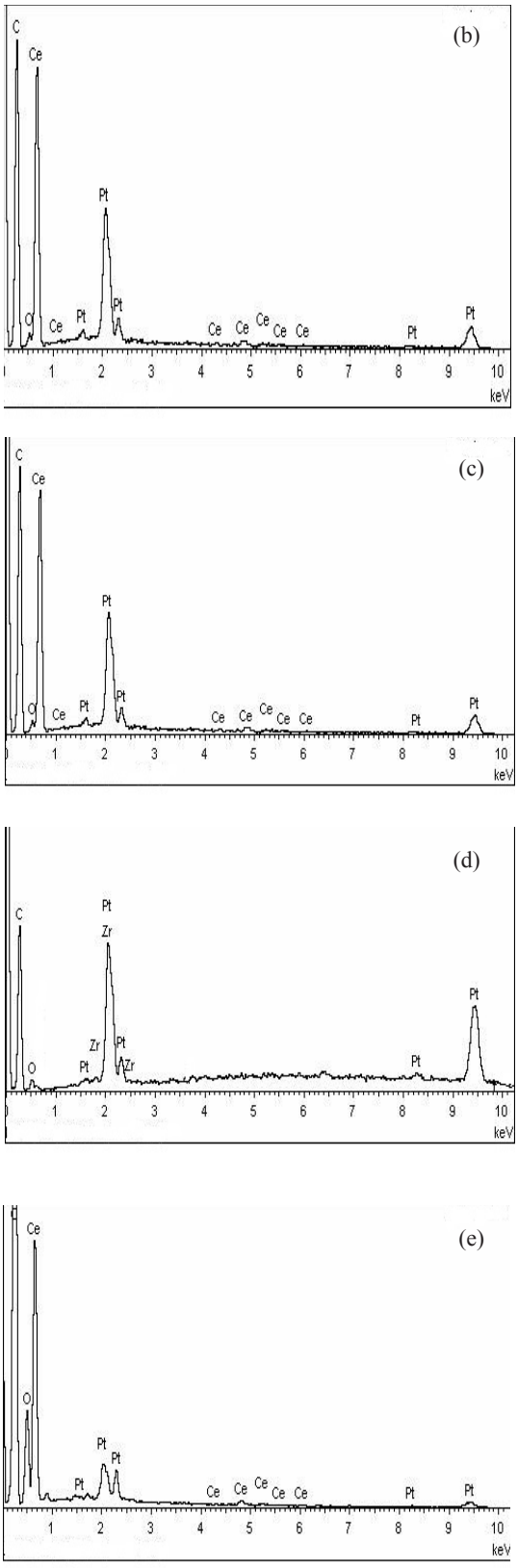

Fig. 2. EDX spectra of (a)Pt/C, (b)Pt−TiO2/C, (c) Pt−CeO2/C, (d) Pt−ZrO2/C and (e) Pt−CeO2/C-1 electrocatalysts.

3 a, a'. A higher degree of particle agglomeration is observed with particle size of 3.57 nm as shown in Table 3. Figure (3b& 3b') display TEM images of Pt–TiO_2/C electrocatalyst. The catalyst particles were homogeneously dispersed on the carbon support in with Pt particle size of 3.06 nm. (Fig.3c&3c') Figure(3e& 3e') show TEM images of Pt-CeO_2/C and Pt-CeO_2/C-1, respectively. The addition of CeO_2 to Pt/C using a single reducing agent of (EG)during the reduction step decreases the resultant Pt particle size (2.50 nm) while using mixed reducing agent (EG +$NaBH_4$) increases Pt particle size (2.78 nm) which in agreement with the fact that; the used reducing agent strongly affects morphology and ORR activity of nano carbon supported electrocatalysts. Using different reducing agents, namely; ethylene glycol (EG), borohydride ($NaBH_4$) and formaldehyde (HCHO) resulted in producing electrocatalysts with different particle size. The method with (EG) has resulted in the smallest mean particle sizes in the range between 4.6 and 6.6 nm, the electrocatalyst based on $NaBH_4$ provided the mean particle size ranging between 4.6 and 13.3 nm, while that based on HCHO has showed a mean particle size in the range 8.8 - 22.9 nm[51].When CeO2 is added to Pt/C in Pt-CeO_2/C electrocatalyst as in Figs. 3c,c' aggregated particles are shown, this could be attributed to the tendency of Pt-CeO_2 nanoparticles to form agglomerates[52]. TEM images of Pt-ZrO_2/C electrocatalystare represented in Figs. (3d&3d') Pt particle size was found to be 3.49 nm which is little bit smaller than that of Pt/C (3.57 nm), this is somewhat similar to results obtained by Liu et al. who found that; The particle size for Pt/C catalyst is 3.0 nm while that of Pt_4ZrO_2/C catalyst is 4.2 nm(31).

Electrochemical characterization

Electrochemical surface area (ECSA) evaluation

The electrochemical active surface area

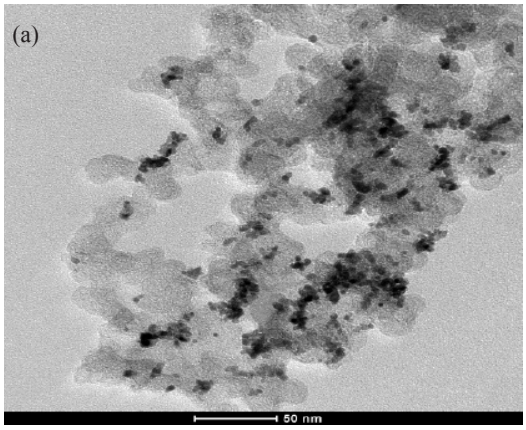

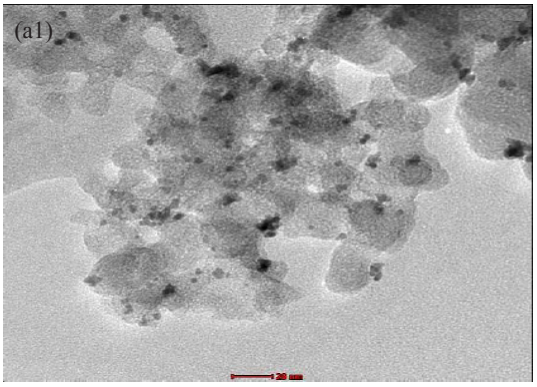

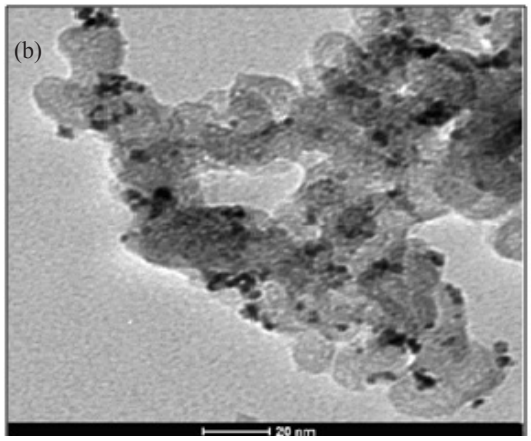

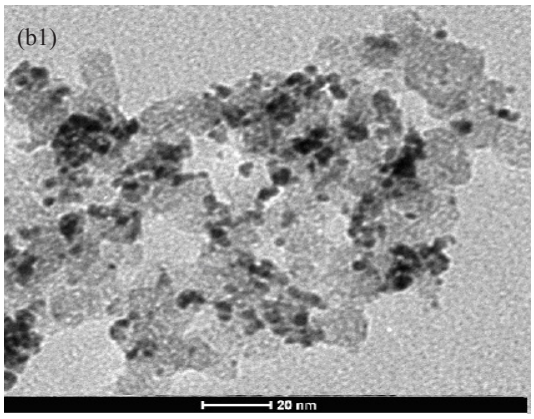

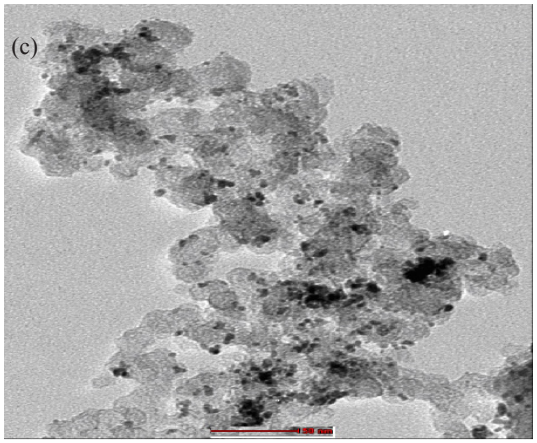

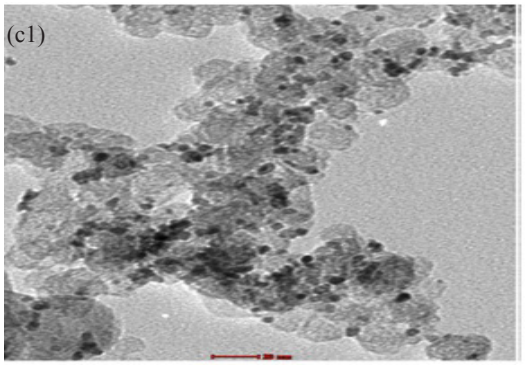

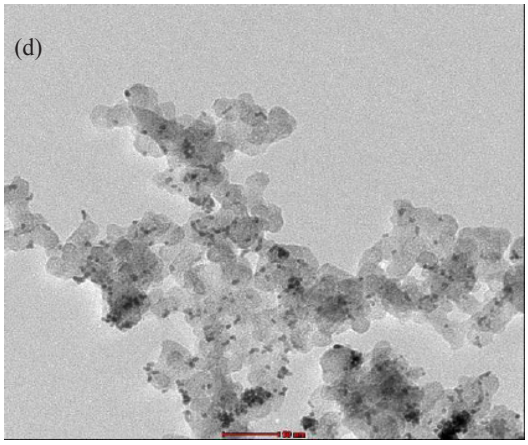

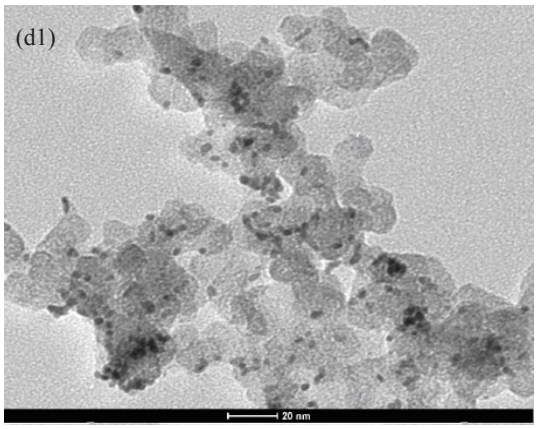

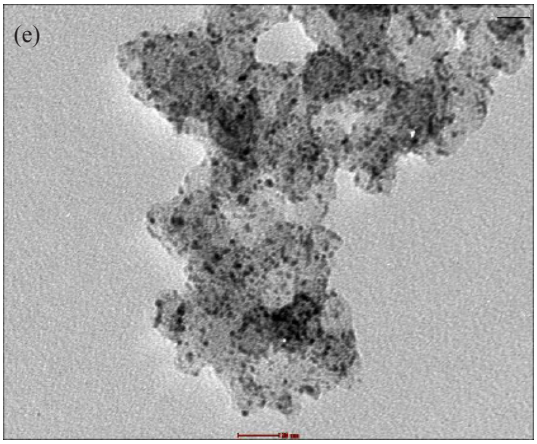

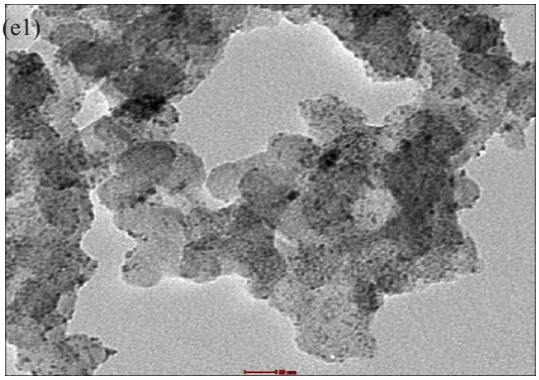

Fig. 3. TEM images of (a,a1) Pt/C, (b, b1)Pt−TiO_2/C, (c, c1) Pt−CeO_2/C, (d, d1) Pt−ZrO_2/C and (e, e1) Pt−CeO_2/C-1electrocatalysts.

(ECSA) of a catalyst is calculated according to the following equation[53, 54]:

$$\text{ECSA } (m^2g^{-1}) = \qquad (1)$$

where QH (C m^{-2}) is the charge of hydrogen desorption, [Pt] (g m^{-2}) is the quantity of Pt loading on the electrode.

ECSA of the prepared electrocatalysts was estimated by integrating the voltammograms corresponding to hydrogen adsorption−desorption area. It is so obvious from Fig.4 that all Pt-MO_x/C have higher ECSA values than that of Pt/C as shown in Table 4 which is could be due to the presence of more active sites on the Pt-MO_x/C surfaces than those on Pt/C surface[55].

Pt-ZrO_2/C and Pt-CeO2/C electrocatalyst has the highest ECSA value among all studied electrocatalysts which are 69.60 and 46.93 m^2g^{-1} respectively, but in case of Pt-TiO_2/C, it was noticed that; although its mass activity at 0.65V/ RHE is -0.567 $mAmg^{-1}$which is smaller than that of Pt/C that equals-2.11$mAmg^{-1}$, it was found to have higher ECSA value, 32.90 m^2g^{-1} than that of Pt/C which is 24.60 m2g-1, this could be attributed to the smaller Pt size of Pt-TiO_2/C (3.06 nm) if it has been compared to Pt/C (3.57 nm) and better Pt dispersion as seen in Fig.(3a, 3a' and 3 b, 3b').This is in accordance with Gustavsson et al. who showed that the presence of TiO_2 can either increase or decrease the ORR performance of Pt catalyst, depending on the sequence through which the thin films have been deposited which comes in accordance with the fact that; synthesis method has been found to make changes in the Pt electronic and geometric parameters[40].

On comparing the two prepared Pt-CeO_2/C; namely: Pt-CeO_2/C and Pt-CeO_2/C-1 we noticed that, changing the used reducing agent affects the behavior of the resultant electrocatalyst, as calculated from Equation 1, Pt-CeO_2/C showed higher ECSA value that equals 46.93 m^2g^{-1} than that of Pt-CeO_2/C-1; 39.85 m^2g^{-1}. Another observation is related to both Pt-ZrO_2 carbon supported electrocatalyst which is although it has large particle size (3.49 nm) it showed the highest ECSA and electrocatalytic activity, this could be explained by the fact that the difference in particle size is not huge to the extent that affects its catalytic activity if compared to results obtained by Oishi and Savadogo who synthesized Pd electro-catalyst monolayer on different single crystal substrates which was found to have wide range of particle sizes up to 92 nm with mean value of 18–20 nm[56].

Cyclic voltammetry results

Cyclic Voltammograms curves (CVs) in oxygen saturated solution were recorded in the potential range from -1.0 to 1199 mV/RHE. The results of Pt/C and Pt-MOx/C catalysts are presented in Fig. 5, the voltammograms shape is the typical shape of that of Pt nanoparticles in acid medium[57, 58]. Pt/C, Pt-TiO_2/C and Pt-CeO_2/C electrocatalysts show:

- The characteristic H adsorption- desorption peak at 0.05-0.3 V/RHE while that for Pt-ZrO_2/C lies at 0.05-0.4 V/RHE.
- Pt oxide formation-reduction peaks at 0.85/0.60 V/RHE.
- It could be easily noticing that; Pt-ZrO_2/C and Pt-CeO_2/C have the highest Pt oxidation-reduction peaks among the prepared electrocatalysts

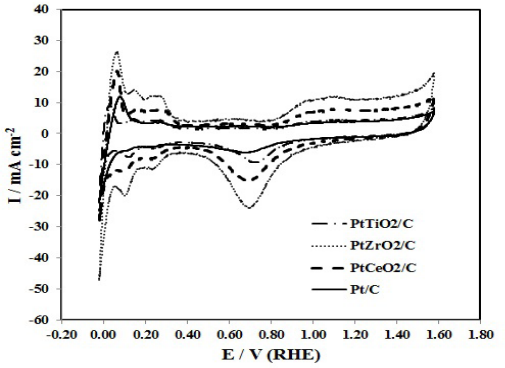

Fig. 4. 30th C.V.s of Pt/C and different Pt-MOx/C electrocatalysts in 0.5 M H_2SO_4 solution at 25 °C; scan rate: 50 mVs^{-1}

Study of oxygen reduction with RDE

Figure6 represents linear sweep voltammograms (LSVs) of Pt/C and Pt-MOx/C where (M = Ti, Ce or Zr), it is obvious that, all prepared Pt-MO_x/C electrocatalysts have higher activity towards ORR than Pt/C except for Pt-TiO_2/C. Moreover Pt-ZrO_2/Chas the highest mass activity values at 0.65V/RHE that equals -9.75 $mAmg^{-1}$ *i.e.* the best activity towards ORR when it was compared with the other catalysts, this is because ZrO_2 was found to have fairly high oxygen storage capacity, which enlarges the oxygen concentration at the catalyst surface, and achieves higher ORR activity with maintaining the catalyst at the same oxygen pressure[59].

Regarding forPt-CeO_2/C; it has high activity for ORR as seen from Fig. 6 and shows a good catalytic activity for ORR; -2.240 $mAcm^{-2}$ at

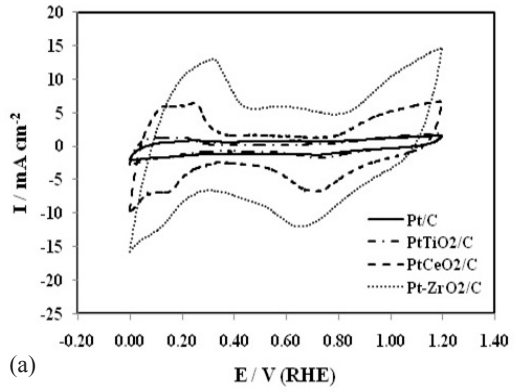

(a)

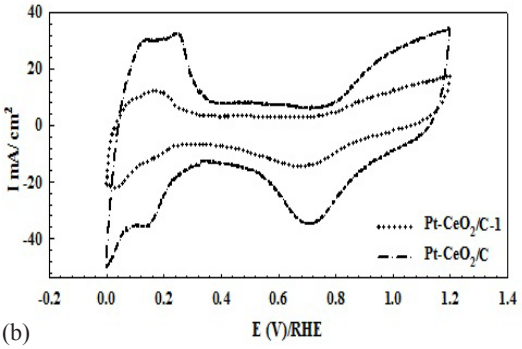

(b)

Fig. 5. Cyclic voltammograms of (a) Pt/C and different Pt-MOx/C, (b) Pt- CeO_2 /C and Pt-CeO_2 /C-1 electrocatalysts in O_2 saturated 0.5 M H_2SO_4 solution at 25 °C; scan rate: 50 mVs^{-1}.

0.65V/RHE which is higher than that of Pt/C(-1.262mAcm^{-2}) at the same potential value as seen in Table 4, this could be interpreted in the light of the fact that; Pt-CeO_x appears to have a characteristic system when compared to other Pt−oxide composite catalysts; the active oxygen supplied from CeO_2 to Pt surface contributed to the improvement of the ORR activity of the Pt-CeO_x cathode, so this noticed behaviour of high ORR activity of Pt-CeO_2/C may be improved by formation of Pt surface partially covered by amorphous Ce_2O_3 layer or may be due to the role of ceria layer in Pt oxide formation on Pt[60].

On evaluating the performance of mentioned electrocatalysts prepared using the mixed

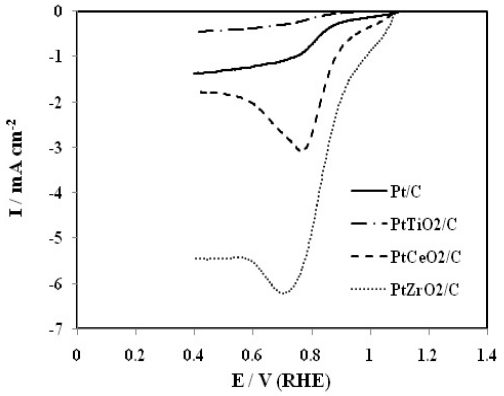

Fig. 6. RDE voltammograms of Pt/C and different Pt-MOx/C electrocatalysts with electrode rotation rate at 2400 rpm in O_2 saturated 0.5 M H_2SO_4 solution at 25 ^oC; scan rate: 10 mVs^{-1}.

reducing agent, it was found that Pt–CeO2/Chas a higher potential value; 1097.9 mV/RHE than that of Pt-TiO2/C; 967.9 mV/RHE at zero current, this big difference which equals 130.0 mV is related to the difference in mass activity value at 0.65V/RHE which is -2.240 mAcm-2 for Pt-CeO2/C and -0.340 mAcm-2 for Pt-TiO2/C, meaning that increasing in the mass activity value of Pt−CeO2/C 6.588 times as that of Pt-TiO2/C. The case is different for Pt−ZrO2/C in which the mass activity value at 0.65V/RHE is the highest among the studied Pt-MOx/C; -5.840 mAcm-2. The onset potential is known as the potential at which the current for oxygen reduction is first observed[61]. Here the onset potential value for Pt−ZrO2/C is the highest one among the studied electrocatalysts; 1041.2 mV/RHE indicating that the oxygen reduction catalytic activity of this electrocatalyst exceeds the other catalysts regarding to onset potential values; the higher onset potential values the higher catalytic activity towards ORR[62] as seen from Fig 6.

Figure 7 (a, b) shows the (LSVs) of ORR on the Pt-CeO_2/C and Pt-CeO_2/C-1 electrodes respectively in O_2 saturated 0.5 M H_2SO_4 solution with rotation rates ranging between 200-2400 rpm.

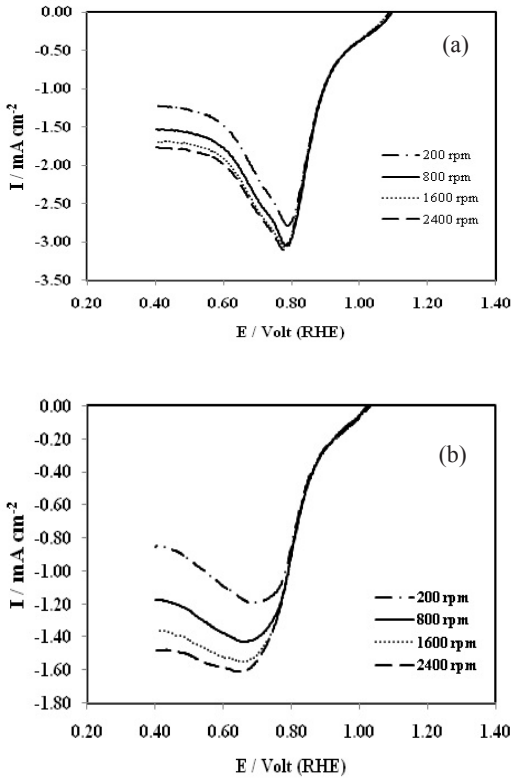

Fig. 7. RDE voltammograms of (a) Pt- CeO_2 /C, (b) Pt- CeO_2 /C-1 with electrode rotation rates at 200, 800, 1600, and 2400 rpm. Electrode potential window 1.6 V to 0.4 V/RHE, scan rate 10 mVs^{-1}.

Clear performance differences between the two catalysts can be figured out by comparing the LSVs of a particular electrode rotation speed. It is very clear that there is an extrusive relation between cathodic current values and the rate of electrode rotation. The studied catalyst samples show the same ORR open circuit potential (around 1040 mV for Pt-CeO_2/C-1 and around 1080 mV for Pt-CeO_2/C), generally this is in consistent with the expected behavior for ORR in aqueous acid medium catalyzed by Pt nanoparticles on carbon supports[60].

TABLE 2. Weight and atomic percentages of different elements forming Pt/C and different Pt-MO_x/C electrocatalysts

Element	Pt/C		Pt−TiO_2/C		Pt−CeO_2/C		Pt−ZrO_2/C		Pt−CeO_2/C-1	
	Weight%	Atomic%	Weight%	Atomic%	Weight%	Atomic%	Weight%	Atomic%	Weight%	Atomic%
C K	63.97	96.65	42.82	86.70	44.60	89.58	37.69	86.26	67.83	84.19
O K	-	-	2.98	4.54	2.27	3.42	2.80	4.80	15.38	14.34
Pt M	36.03	3.35	48.96	6.10	44.29	5.48	56.03	7.89	10.39	0.79
Ti K	-	-	5.24	2.66	-	-		-	-	-
Ce L	-	-	-	-	8.84	1.52	-		6.40	0.68
Zr L	-	-	-	-			3.48	1.05	-	-

TABLE 3. Particle size values of Pt/C and different Pt-MO_x/C electrocatalysts according to TEM analysis.

Electrocatalyst	Particle size / nm
Pt/C	3.57
Pt-TiO_2/C	3.06
Pt-CeO_2/C	2.78
Pt-ZrO_2/C	3.49
Pt-CeO_2/C-1	2.50

TABLE 4. Electrochemical parameters and electrochemical surface area values obtained from LSVs and CVs of Pt/C and Pt-Mo_x/C electrocatalysts 0.5 MH_2SO_4 solution.

Electrocatalysts	Open circuit pot. [mV/RHE] at 0 current	Onset ORR [mV/ RHE]	ECSA [m^2g^{-1}]	Current density at 650 mV/RHE
Pt/C	899.5	830.1	24.60	-1.262
Pt-TiO_2/C	967.9	790.5	32.90	-0.34
Pt-CeO_2/C	1097.9	931.4	46.93	-2.240
Pt-ZrO_2/C	801.0	1041.2	69.60	-5.840

The increase in the diffusion limiting current in the RDE measurement is directly proportional to the rotation speed. The limiting current densities of Pt-CeO_2/C increased from 1.25 to 1.80 $mAcm^{-2}$while that of Pt-CeO_2/C-1 increased from 0.82 to 1.55 $mAcm^{-2}$ as the rotation speeds were increased from 200 to 2400 rpm, this behavior could be explained by the fact that; higher rotation speeds leads to faster oxygen flux at the electrode surface and hence generating higher currents.

Hydrated oxide reduction produced by applying a reducing agent. Typical reducing agents are H_2 [63] where strength of reduction is controlled by temperature [64, 65] and $NaBH_4$ [66] which have strong reduction strength at room temperature

Comparing Pt-CeO_2/C and Pt-CeO_2/C-1 in Fig. (7a, 7b) we can easily notice that, for 2400 rpm, Pt-CeO_2/C had a higher current density value at 0.65V/RHE; -2.240 $mAcm^{-2}$ than that of Pt-CeO_2/C-1 that equals to-1.597 $mAcm^{-2}$, this could be related to the fact that, smaller particle sized electrocatalysts produced from using single reducing agent may tend to agglomerate and hence reduce the activity of the whole electrocatalysts, hence the oxide reduction extent in the preparation method affects the Pd and Au performance towards the ORR which is related to the catalyst synthesis procedures [67-71].

From the comparison of the LSVs recorded for both Pt-CeO2 on Carbon catalysts at 2400 rpm we can easily also observe the differences in the open circuit potential,limiting currentand half wave potential values. The open circuit potential is higher in case of Pt-CeO_2/C catalyst; 1097.9 mV/RHE than in case of Pt-CeO_2/C-1; -1055.3 mV/RHE, faster ORR is observed in the whole potential window for Pt-CeO_2/C than on Pt-CeO_2/C-1 catalyst. The half wave potential of Pt-CeO_2/C was shifted to about 100 mV in the positive side compared to Pt-CeO_2/C-1. Similarly, the limiting current of Pt-CeO_2/C catalyst is higher by about 300 mA (regardless to the sign) compared to Pt-CeO_2/C-1. The favorable shifts in the open circuit, half wave potential and limiting current regions equivalent to the electrode of Pt-CeO2/C can be attributed to the enhanced ORR activity. It was found that the difference in the limiting currents for the two electrocatalysts may

be due to the difference of oxygen diffusion at both of them[72]. It is also found that Pt-CeO_2/C (8.84 Ce%) had higher onset potential and limiting current than Pt-CeO_2/C-1 (6.40 Ce%) which is in accordance with Kang et al.[73]

Oxygen reduction mechanism of Pt-CeO2/C and Pt-CeO_2/C-1 has been evaluated using the Koutecky-Levichequation to determine the number of electrons transferred per O_2 molecule.

$$-\frac{1}{I} = -\frac{1}{I_k} + \frac{1}{0.62\, n\, FAD^{1/2} cv^{-1/6} \omega^{1/2}} \quad (2)$$

where I_k is the kinetic current; ω is the rotation rate; n is the number of electrons involved in the reaction; F is Faraday constant; A is the geometric area of the disk electrode; D and c are the diffusion coefficient of dissolved oxygen and the concentration of dissolved oxygen in 0.5M H_2SO_4, respectively; v is the kinematic viscosity of the electrolyte.

Figure 8 a, b represents Koutecky-Levitch (-1/I versus $\omega^{-1/2}$) plots for the ORR on Pt-CeO_2/C and Pt-CeO_2/C-1 electrodes respectively at electrode potential range from 0.2V - 0.5V vs. RHE in 0.5M H_2SO_4. The linearity and the parallism of these plots indicate first-order kinetics with respect to molecular oxygen[74]. The calculation of n was performed using the values: F= 96,485 $Cmol^{-1}$; A= 0.196 cm^2; D = 1.93×10^{-5} cm^2 s^{-1}; c =1.13×10^{-6} mol cm^{-3}; v=9.5×10-3 cm^2 s^{-1}[75]. Intercept different values at the y-axis indicate the existence of different kinetic constants at different electrode potentials while the non-zero values of the intercepts imply that the ORR is not controlled solely by diffusion [76].

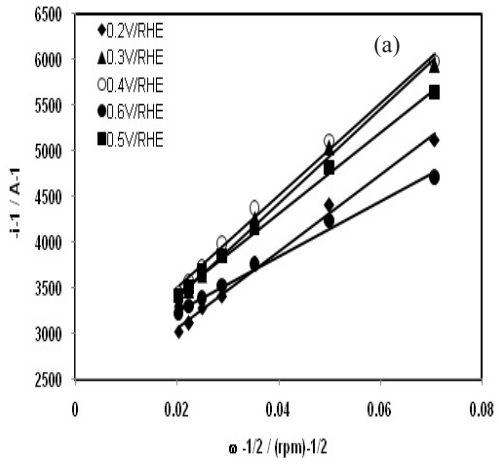

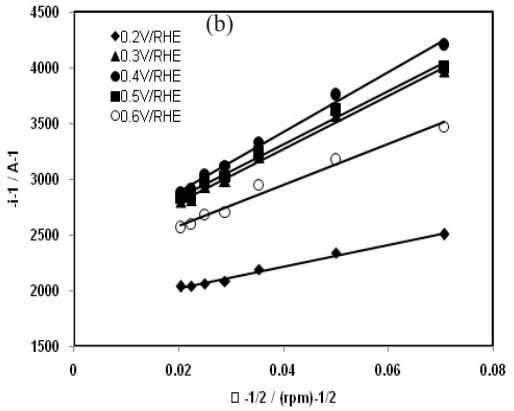

Fig. 8.Koutecky–Levichplot drawn at different potentials for (a) Pt- CeO_2/C, b) Pt- CeO_2 /C-1 in O_2-saturated 0.5 M sulphuric acid solution at 2400 rpm, scan rate 10 mVs^{-1}.

Conclusion

Pt-MO_x/C electrocatalysts have been prepared through two steps. The first step involves the synthesis of MOx/C powders via solid state reaction under intermittent microwave heating, while the second step is platinum loading on MO_x/C surfaces using ethylene glycol or a mixture of ethylene glycol and sodium borohydride as the reducing agent.

- The preparation method of the electrocatalysts is found to affect their behaviour towards ORR.
- Pt-CeO_2/C and Pt-ZrO_2/C have the highest activity for oxygen reduction among the studied electrocatalysts and also higher than that of prepared Pt/C in acid medium.
- Changing the used reducing agent was found to affect the electrocatalytic efficiency and electrochemical surface area of the resultant electrocatalyst.
- Pt-CeO_2/C and Pt-CeO_2/C-1 showed first-order kinetics with respect to molecular oxygen with oxygen reduction reaction not controlled solely by diffusion.

References

1. Jiang, T., Brisard, G.M., Determination of the kinetic parameters of oxygen reduction on copper using a rotating ring single crystal disk assembly (RRDCu(hkl)E). *Electrochim Acta.* **52,** 4487-96, (2007).

2. Marković, N.M., Schmidt, T.J., Stamenković, V., Ross, P.N., Oxygen reduction reaction on pt and pt bimetallic surfaces: A selective review. *Fuel Cells.* **1,** 105–16, (2001).

3. Neergat, M., Shukla, A.K., Gandhi, K.S., Platinum-based Alloys as oxygen–reduction Catalysts for Solid–Polymer–Electrolyte Direct Methanol Fuel Cells. *J. Appl Electrochem.* **31,** 373–8. (2001).

4. Toda, T., Igarashi, H., Uchida, H., Watanabe, M., Enhancement of the Electroreduction of Oxygen on Pt Alloys with Fe, Ni, and Co. *J. Electrochem Soc.* **146,** 3750-6 .(1999).

5. Li, W., Zhou, W., Li, H., Zhou, Z., Zhou, B., Sun, G., et al. Nano-stuctured Pt–Fe/C as cathode catalyst in direct methanol fuel cell. *Electrochim Acta.* **49,** 1045–55. (2004).

6. Ehteshami, S.M.M., Chan, S.H., A review of electrocatalysts with enhanced CO tolerance and stability for polymer electrolyte membarane fuel cells. *Electrochim Acta.* **93,** 334–45. (2013).

7. Liaxg, C.C., Juliard, A.L., The overpotential of oxygen reduction at platinum electrodes. *J Electroanal Chem.* **9,** 390–4. (1965).

8. Rosalbino, F., Delsante, S., Borzone, G., Angelini, E., Electrocatalytic behaviour of Co–Ni–R (R=Rare earth metal) crystalline alloys as electrode materials for hydrogen evolution reaction in alkaline medium. *Int J. Hydrogen Energy.* **33,** p. 6696–703. (2008).

9. Jaks, M.M., Hypo – hyper- d -electronic interactive nature of synergism in catalysis and electrocatalysis for hydrogen reactions. **45,** 4085–99. (2000).

10. Neophytides, S.G., Murase, K., Zafeiratos, S., Papakonstantinou, G., Paloukis, F.E., Krstajic, N.V., et al. Composite hypo-hyper-d-intermetallic and interionic phases as supported interactive electrocatalysts. *J. Phys Chem B.* **110,** p. 3030–42. (2006).

11. Jakšić, M.M., Hypo-hyper-d-electronic interactive nature of interionic synergism in catalysis and electrocatalysis for hydrogen reactions. *Int J. Hydrogen Energy.* **26,** p. 559–78. (2001).

12. Wang, X., Xu, W., Zhou, X., Lu, T., Xing, W., Liu, C., et al. PtCeOx/C as a novel methanol-tolerant electrocatalyst of oxygen reduction for direct methanol fuel cells. *J. Solid State Electrochem.* **13,** 1449–53. (2009).

13. Xu, F., Xu, R., Mu, S., Enhanced SO_2 and CO poisoning resistance of CeO_2 modified Pt/C catalysts applied in PEM fuel cells. *Electrochim Acta.* **112,** 304–9. (2013).

14. Lim, D.H., Lee, W.D., Choi, D.H., Lee, H.I., Effect of ceria nanoparticles into the Pt/C catalyst as cathode material on the electrocatalytic activity and durability for low-temperature fuel cell. *Appl Catal B Environ.* **94,** 85–96. (2010).

15. He, Q., Mukerjee, S., Zeis, R., Parres-Esclapez, S., Illán-Gómez, M.J., Bueno-Lópeza., Enhanced Pt stability in MO_2 (M=Ce, Zr or Ce0.9Zr0.1)-promoted Pt/C electrocatalysts for oxygen reduction reaction in PAFCs. *Appl Catal A Gen.* **381,** 54–65. (2010).

16. Gu, D.M., Chu, Y.Y., Wang, Z.B., Jiang, Z.Z., Yin, G.P., Liu, Y., Methanol oxidation on Pt/CeO_2–C electrocatalyst prepared by microwave-assisted ethylene glycol process. *Appl Catal B Environ.* **102,** 9–18.(2011).

17. Scibioh, M.A., Kim, S.K., Cho, E.A., Lim, T.H., Hong, S.A., Ha, H.Y., Pt-CeO_2/C anode catalyst for direct methanol fuel cells. *Appl Catal B Environ.* **84,** 773–82. (2008).

18. Xu, C., Shen, P.K., Electrochamical oxidation of ethanol on Pt-CeO_2/C catalysts. *J. Power Sources.* **142,** 27–9. (2005).

19. Xu, C., Zeng, R., Shen, P.K., Wei, Z., Synergistic effect of CeO_2 modified Pt/C catalysts on the alcohols oxidation. *Electrochim Acta.* **51,** 1031–5. (2005).

20. Peng, W., Zhao, L., Zhang, C., Yan, Y., Xian, Y., Controlled growth cerium oxide nanoparticles on reduced grapheme oxide for oxygen catalytic reduction. *Electrochim Acta.* **191,** 669-76, (2016).

21. Guo, X., Guo, D.J., Qiu, X.P., Chen, L.Q., Zhu, W.T., Excellent dispersion and electrocatalytic properties of Pt nanoparticles supported on novel porous anatase TiO_2 nanorods. *J. Power Sources.* **194,** 281–5. (2009).

22. Selvaganesh, S.V., Selvarani, G., Sridhar, P., Pitchumani, S., Shuklaa., K., A durable PEFC with carbon-supported Pt–TiO[sub 2] cathode: A cause and effect study. *J. Electrochem Soc.* **157,** B1000. (2010).

23. Ruiz-Camacho, B., Valenzuela M.A., González-Huerta, R.G., Suarez-Alcantara, K., Canton, S.E., Pola-Albores, F., Electrochemical and XAS investigation of oxygen reduction reaction on Pt-TiO_2-C catalysts. *Int J. Hydrogen Energy.* **38,**12648–56. (2013).

24. De Tacconi, N.R., Chenthamarakshan, C.R., Rajeshwar, K., Lin, W.Y., Carlson, T.F., Nikiel L, et al. Photocatalytically generated Pt/C–TiO[sub 2] electrocatalysts with enhanced catalyst dispersion for improved membrane durability in polymer electrolyte fuel cells. *J. Electrochem Soc.* **155,** B1102. (2008).

25. Jeon, M.K., McGinn, P.J., Effect of Ti addition to Pt/C catalyst on methanol electro-oxidation and oxygen electro-reduction reactions. *J. Power Sources.* **195,** 2664–8. (2010).

26. Mukerjee, S., Role of structural and electronic properties of Pt and Pt alloys on electrocatalysis of oxygen reduction. *J. Electrochem Soc.* **142,** B1409. (1995).

27. Hayashi, T., Ishihara, A, Nagai, T., Arao, M., Imai, H., Kohno, Y., Matsuzawa, K., Mitsushima, S., Ota, K., Temperature dependence of oxygen reduction mechanism on a titanium oxide–based catalyst made from oxy–titanium tetra– pyrazino–porphyrazine using carbon nano-tubes as support in acidic solution. *Electrochim Acta.* **209,** p.1-6, (2016).

28. Ando, F., Tanabe, T., Gunji, T., Tsuda, T., Kaneko, S., Takeda, T., Ohsaka, T., Matsumoto, F., Improvement of ORR activity and durability of Pt electrocatalyst nanoparticles anchored on TiO_2/cup-stacked carbon nanotube in acidic aqueous media. *Electrochim Acta.* **232,** 404-13(2017).

29. Esfahani, R.A.M., Vankova, S.K., Videla, A.H.A.M., Specchia, S., Innovative carbon-free low content Pt catalyst supported on Mo-doped titanium suboxide (Ti_3O_5-Mo) for stable and durable oxygen reduction reaction. *Appl Catal B Environ.* **201,** 419–29, (2017).

30. Wang, R., Wang, K., Wang, H., Wang, Q., Key, J., Linkov, V., et al. Nitrogen-doped carbon coated ZrO_2 as a support for Pt nanoparticles in the oxygen reduction reaction. *Int J. Hydrogen Energy.* **38,** 5783–8. (2013).

31. Liu, G., Zhang, H., Zhai, Y., Zhang, Y., Xu, D., Shao, Z., Pt_4ZrO_2/C cathode catalyst for improved durability in high temperature PEMFC based on H_3PO_4 doped PBI. *Electrochem Commun.* **9,** 135–41. (2007).

32. Shahid, M.M., Rameshkumar, P, Basirun, W.J., Ching, J.J., Huang, N.M., Cobalt oxide nanocubes interleaved reduced graphene oxide as an efficient electrocatalyst for oxygen reduction reaction in alkaline medium. *Electrochim Acta.* **237,** 61-8, (2017).

33. Wang, Q., Hu, W., Huang, W., Nitrogen doped graphene anchored cobalt oxides efficiently bi-functionally catalyze both oxygen reduction reaction and oxygen revolution reaction. *Int J. Hydrogen Energy.* **42,** p. 5899–907, (2017).

34. Chen, W., Zhao, J., Yang, L.J., Liu, Z., Microwave heated polyol synthesis of carbon nanotubes supported Pt nanoparticles for methanol electrooxidation. *Materials Chemistry and Physics.* **91**, 124–9, (2005).

35. Zhao, J., Chen, W., Zheng, Y., Li, X., Xu, Z., Microwave polyol synthesis of Pt/C catalysts with size controlled Pt particles for methanol electrocatalytic oxidation. *Journal of Material Science.* **41,** 5514–8, (2006).

36. Suguru, Y., Masahito, S., Microwave-assisted chemical modification of carbon nanohorns: oxidation and Pt deposition. *Chemical Physics Letters.* **433,** p. 97–100, (2006).

37. Peuchert, M., Yoneda, T., Betta, R., Boudart, M., Oxygen reduction on small supported platinum particles. *Journal of Electrochemica Society*. **5, 133**, 944 -7, (1986).

38. Kinoshita, K., Particle size effects for oxygen reduction on highly dispersed platinum in acid electrolytes. *Journal of the Electrochemical Society.* **3,** 137, 845-8, (1990).

39. Takasu, Y., Itaya, H., Iwazaki, T., Miyoshi, R., Ohnuma, T., Sugimoto, W., Murakami, Y., Size effects of ultrafine Pt-Ru particles on the electrocatalytic oxidation of methanol. *Chemical Communications*. 2001, 341-2, (2001).

40. Meng, H., Shen, P.K., The beneficial effect of the addition of tungsten carbides to Pt catalysts on the oxygen electroreduction. *Chem Commun.* **41,** 35 4408-10, (2005).

41. Tian, Z.Q., Xie, F.Y., Shen, P.K., Preparation of high loading Pt supported on carbon by on-site reduction. *J. Mater Sci.* **39,** 4: p. 1507-9, (2004).

42. Shen, P.K., Tian, Z., Performance of highly dispersed Pt/C catalysts for low temperature fuel cells. *Electrochim Acta.* **49,** 19: p.3107-11, (2004).

43. Xu, C., Shen, P.K., Novel Pt/CeO_2/C catalysts for electrooxidation of alcohols in alkaline media. *Chem Commun.* **40,** 19: 2238-9, (2004).

44. Lim, D.H., Lee, W.D., Choi, D.H., Kwon, H.H., Lee, H.I., The effect of cerium oxide nanoparticles on a Pt/C electrocatalyst synthesized by a continuous two-step process for low-temperature fuel cell. *Electrochem Commun*. **10,** 592–6. (2008).

45. Justin, P., Hari, K., C., P., Ranga, R., G., High performance Pt–Nb_2O_5/C electrocatalysts for methanol electrooxidation in acidic media. *Appl Catal B Environ.* **100,** 510–5. (2010).

46. Justin, P., Rao, G.R., Enhanced activity of methanol electro-oxidation on Pt–V_2O_5/C catalysts. *Catal Today.* **141,** 138–43. (2009).

47. Zhou, C., Wang, H., Peng, F., Liang, J., Yu, H., Yang, J., MnO_2/CNT supported Pt and PtRu nanocatalysts for direct methanol fuel cells. *Langmuir.* **25,** 7711–7.(2009).

48. Saha, M.S., Li, R., Cai, M., Sun, X., High electrocatalytic activity of platinum nanoparticles on SnO_2 nanowire-based electrodes. *Electrochem Solid State Lett.* **10,** B130. (2007).

49. Maheswari S, Sridhar P, Pitchumani S. Pd–

TiO_2/C as a methanol tolerant catalyst for oxygen reduction reaction in alkaline medium. *Electrochem Commun.* **26,** 97–100. (2013)

50. Hyde, T., Final analysis: Crystallite size analysis of supported platinum catalysts by xrd. *Platin Met Rev.* **52,** 129–30. (2008).

51. Zhang, L., Lee, K.C., Zhang, J.J., Effect of synthetic reducing agents on morphology and ORR activity of carbon-supported nano-Pd-Co alloy electrocatalysts, *Electrochimica Acta.* **52,**7964–71. (2007).

52. Altamirano-Gutiérrez, A., Fernández, A.M., Rodríguez Varela, F.J., Preparation and characterization of Pt-CeO_2 and Pt-Pd electrocatalysts for the oxygen reduction reaction in the absence and presence of methanol in alkaline medium. *Int J. Hydrogen Energy.* **38**,12657–66. (2013).

53. Zhu, H., Li, X., Wang, F., Synthesis and characterization of Cu@Pt/C core-shell structured catalysts for proton exchange membrane fuel cell. *Int J. Hydrogen Energy.* **36,** 9151–4 (2011).

54. Yu, S., Lou, Q., Han, K., Wang, Z., Zhu, H., Synthesis and electrocatalytic performance of MWCNT-supported Ag@Pt core–shell nanoparticles for ORR. *Int J. Hydrogen Energy.* **37,** 13365–70.(2012).

55. Ruiz-Camacho, B., Martínez-Álvarez, O., Rodríguez-Santoyo, H.H., Granados-Alejo, V., Pt/C and Pt/TiO_2–C electrocatalysts prepared by chemical vapor deposition with high tolerance to alcohols in oxygen reduction reaction. *J Electroanal Chem.* **725,** 19–24. (2014).

56. Oishi, K., Savadogo, O., Correlation between the physico-chemical properties and the oxygen reduction reaction electro catalytic activity in acid medium of Pd–Co alloys synthesized by ultrasonic spray method. *Electrochimica Acta.* **98,** 225–38. (2013).

57. Tiido, K., Alexeyeva, N., Couillard, M., Bock, C., MacDougall, B.R., Tammeveski, K., Graphene-TiO_2 composite supported Pt electrocatalyst for oxygen reduction reaction. *Electrochim Acta.* **107,** 509–17. (2013).

58. Elezovic, N.R., Babic, B.M., Radmilovic, V.R., Vracar, L.M., Krstajic, N. V., Synthesis and characterization of MoOx-Pt/C and TiOx-Pt/C nano-catalysts for oxygen reduction. *Electrochim Acta.* **54,** 2404–9. (2009).

59. Xu, Z., Qi, Z., Kaufman, A., Effect of oxygen storage materials on the performance of proton-exchange membrane fuel cells. *J. Power Sources.* **115,** 40–3.(2003).

60. Fugane, K., Mori, T., Ou, D.R., Suzuki, A., Yoshikawa, H., Masuda, T., et al. Activity of oxygen reduction reaction on small amount of amorphous CeO x promoted Pt cathode for fuel cell application. *Electrochim Acta*. **56,** 3874–83. (2011).

61. Asteazaran, M., Bengio, S., Triaca, W.E., Castro, L. AM., Methanol tolerant electrocatalysts for the oxygen reduction reaction. *J. Appl Electrochem.***44,** 1271–78. (2014).

62. Chung, H.T., Won, J.H., Zelenay, P., Active and stable carbon nanotube /nanoparticle composite electrocatalyst for oxygen reduction. *Nature Communications*. **4,** Article number: 1922. (2013).

63. Moss, R.L., Preparation and Characterization of Supported Metal Catalysts, in: Anderson RB, Dawson PT (Eds.), *Experimental Methods in Catalytic Research,* Vol. 2, Ch. 2, Academic Press, New York, p. 43. (1976).

64. Yang, J.H., Henao, J.D., Costello, C., Kung, M.C., Kung, H.H., Miller, J.T., Kropf, A.J., Kim, J.G., Regalbuto, J.R., Bore, M.T., Pham, H.N., Datye, A.K. , Laeger, J.D., Kharas, K., Understanding preparation variables in the synthesis of Au/Al_2O_3 using EXAFS and electronmicroscopy. *Appl.Catal*. A291.73–84. (2005).

65. Wu, S.H., Zheng, X.C., Wang, S.R., Han, D.Z., Huang, W.P., Zhang, S.M., TiO_2 supported nano-Au catalysts prepared via solvated metal atom impregnation for low temperature CO oxidation. *Catal. Letters.* **97,** 17–23. (2004).

66. Liu, Y., Male, P., Bouvrette, P., Luong, J.H.T., Control of the size and distribution of gold nanoparticles by unmodified cyclodextrins. *Chem. Mater.* **15,** 4172–80. (2003).

67. Fernández, J.L., Walsh, D.A., Bard,A.J., Thermodynamic guidelines for the design of bimetallic catalysts for oxygen electro reduction and rapid screening by scanning electrochemical microscopy. M−Co (M: Pd, Ag, Au) *J. Am. Chem. Soc.* **127,** 357–65. (2005).

68. Fernández, J.L., Bard, A.J., Scanning electrochemical microscopy. 47. Imaging electrocatalytic activity for oxygen reduction in an acidic medium by the tip generation-substrate collection mode, *Anal. Chem.* **75,** 2967–74. (2003).

69. Lopez, J.R., Zoski, C.G., Bard. A.J., A.J. Bard, M.V. Mirkin (Eds.), *Scanning Electrochemical Microscopy,* 2nd ed., CH16, Taylor and Francis, *N.Y.* p. 525–68. (2012).

70. Amemiya, S., Bard, A.J., Fan, F.R.F., Mirkin, M.V., Unwin, P.R., Scanning electrochemical

microscopy, *Annu. Rev. Anal. Chem.* **1,** 95–131.; 1: (2008)

71. Fan, F.R.F., Fernandez, J., Liu, B., Mauzeroll, J., Scanning Electrochemical Microscopy, in: C.G.Zoski (Ed.), *Handbook of Electrochemistry,*Ch.12, Elsevier, Amsterdam. 471-540. (2007).

72. Vellacheri, R., Unni, S.M., Nahire, S., Kharul, U.K., Kurungot, S., Pt–MoOx-carbon nanotube redox couple based electrocatalyst as a potential partner with polybenzimidazole membrane for high temperature polymer electrolyte membrane fuel cell applications. *Electrochim Acta.* **55,** 2878-87(2010).

73. Kang, H.L., Kyungjung, K., Victor, R., Duck, Y.Y., Hyuk, C., Doyoung, S., Synthesis and characterization of nanostructured PtCo-CeO_x/C for oxygen reduction reaction. *J. Power Sources.* **185,** 871–85. (2008).

74. Senthil Kumar, S.M., Soler Herrero, J., Irusta, S., Scott, K., The effect of pretreatment of Vulcan XC-72R carbon on morphology and electrochemical oxygen reduction kinetics of supported Pd nano-particle in acidic electrolyte. *J Electroanal Chem.* **647,** 211–21. (2010).

75. El-Deab, M.S., Ohsaka, T., Hydrodynamic voltammetric studies of the oxygen reduction at gold nanoparticles-electrodeposited gold electrodes. *Electrochim Acta.* **47**, 4255-61. (2002).

76. Thanasilp, S., Hunsom, M., Effect of Pt: Pd atomic ratio in Pt-Pd/C electrocatalyst-coated membrane on the electrocatalytic activity of ORR in PEM fuel cells. *Renew Energy*.**36,** 1795–801. (2011).

Received 16/4/2017;
Accepted 21/5/2017)

تحضير و توصيف تراكيب نانومترية من البلاتين و أكاسيد العناصر الانتقالية لتفاعل اختزال الأكسجين في الأوساط الحامضية

كامل محمد محمود الخطيب[١]، أماني عبيد فتوحي[١]، رباب سيد أمين[١] و راندا محمد عبد الحميد[٢]
[١] قسم الهندسة الكيميائية و التجارب نصف الصناعية - المركز القومي للبحوث و[٢] قسم الكيمياء - كلية العلوم - جامعة القاهرة- مصر.

تم تحضير العوامل الحفازة المتكونة من البلاتين و أكاسيد بعض العناصر الانتقالية و المدعمة بالكربون لتطوير عامل حفاز رخيص و فعال لتفاعل اختزال الأكسجين باستخدام عامل مختزل ثنائي (ايثلين جليكول +بوروهيدريد الصوديوم) حيث أن العناصر الانتقالية المستخدمة هي التيتانيوم، السيريوم و الزيركونيوم. تم دراسة البلاتين المدعم بالكربونالمكون من البلاتين و أكسيد السيريوم و المحضر باستخدام الايثلين جليكول منفردا لدراسة تأثير تغير العامل المختزل على نشاط العامل الحفاز لتفاعل اختزال الاكسجين وكذلك حركية تفاعل اختزال الاكسجين. و قد تم تتبع النشاط الحافزي الكهربي للعوامل الحفازة المحضرة لتفاعل اختزال الاكسجين باستخدام الفولتمترية الدائرية و المسح الفولتمتري الخطيعلى الالكترود القرصي الدائري.و قد أظهر العامل الحفاز المكون من البلاتين و أكسيد الزيركونيوم أفضل نشاط لتفاعل اختزال الأكسجين حيث وجد أن كثافة تيار اختزال الأكسجين له (5.840 م أمبير/سم2) حوالي خمسة أضعاف كثافة تيار اختزال الأكسجين عند استخدام البلاتين المدعم بالكربون(1.262 م أمبير/سم2). كما وجد آن العامل الحفاز المكون من البلاتين و أكسيد السيريوم المحضر بعامل مختزل ثنائي له تيار اختزال أكسجين أفضل (2.240 م أمبير/سم2) من نظيره المحضر بالعامل المختزل الأحادي (1.597 م أمبير/سم2) مما يوضح التأثير الكبير لتغيرالعامل المختزل ليس فقط على نشاط العامل الحفازتجاهتفاعل اختزال الأكسجين و انما أيضا على حجم الجسيمات ومحتوى العنصر الانتقالي في العامل الحفاز.أظهرت دراسة حركية تفاعل اختزال الأكسجين للعاملين الحفازين المكونين من البلاتين و أكسيد السيريوم باستخدام معادلة كوشيه ليفيش و أظهرت أنه تفاعل من الدرجة الأولى. تم استخدام حيود الأشعة السينية و الطاقة المتبددة للأشعة السينية و كذلك الميكروسكوب الالكتروني الناقل لتوصيف العوامل الحفازة المحضرة.